

Published in final edited form as:

*Gastroenterology*. 2013 July ; 145(1): 232–241. doi:10.1053/j.gastro.2013.03.047.

## Irbit Mediates Synergy Between Ca<sup>2+</sup> and cAMP Signaling Pathways During Epithelial Transport in Mice

Seonghee Park<sup>1,2</sup>, Nikolay Shcheynikov<sup>1</sup>, Jeong Hee Hong<sup>1</sup>, Changyu Zheng<sup>1</sup>, Suk Hyo Suh<sup>2</sup>, Katsuhiko Kawai<sup>3</sup>, Hideaki Ando<sup>3</sup>, Akihiro Mizutani<sup>4</sup>, Takaya Abe<sup>5</sup>, Hiroshi Kiyonari<sup>5</sup>, George Seki<sup>6</sup>, David Yule<sup>7</sup>, Katsuhiko Mikoshiba<sup>3,8,9</sup>, and Shmuel Muallem<sup>1,8,9</sup>

<sup>1</sup>Epithelial Signaling and Transport Section, Molecular Physiology and Therapeutics Branch, National Institute of Dental and Craniofacial Research, National Institute of Health, Bethesda MD, 20892

<sup>2</sup>Department of Physiology, School of Medicine, Ewha Womans University, 911-1 Mok-6-dong, Yang Chun-gu, Seoul 158-710, Republic of Korea

<sup>3</sup>Laboratory for Developmental Neurobiology, Brain Science Institute, Institute of Physical and Chemical Research (RIKEN), 2-1 Hirosawa, Wako, Saitama 351-0198, Japan

<sup>4</sup>Department of Pharmacotherapeutics, Showa Pharmaceutical University, 3-3165 Higashi-tamagawagakuen, Machida, Tokyo 194-8543

<sup>5</sup>Laboratory for Animal Resources and Genetic Engineering, RIKEN Center for Developmental Biology, 2-2-3 Minatojima Minami, Chuou-ku, Kobe 650-0047

<sup>6</sup>Department of Internal Medicine, Faculty of Medicine, University of Tokyo, 7-3-1 Hongo, Bunkyo-ku, Tokyo 113-8635, Japan

<sup>7</sup>Department of Pharmacology & Physiology, School of Medicine and Dentistry, University of Rochester Medical Center, Rochester, NY, USA

### Abstract

**Background & Aims**—The cAMP and Ca<sup>2+</sup> signaling pathways synergize to regulate many physiological functions. However, little is known about the mechanisms by which these pathways interact. We investigated the synergy between these signaling pathways in mouse pancreatic and salivary gland ducts.

**Methods**—We created mice with disruptions in genes encoding the solute carrier family 26, member 6 (Slc26a6<sup>-/-</sup> mice) and inositol 1,4,5-triphosphate (InsP<sub>3</sub>) receptor-binding protein released with InsP<sub>3</sub> (Irbit<sup>-/-</sup> mice). We investigated fluid secretion by sealed pancreatic ducts and the function of Slc26a6 and the cystic fibrosis transmembrane conductance regulator (CFTR) in

© 2013 The American Gastroenterological Association. Published by Elsevier Inc. All rights reserved.

<sup>8</sup>Address for correspondence: Shmuel.muallem@nih.gov or mikosiba@brain.riken.jp.

<sup>9</sup>KM is the contact person for the IRBIT<sup>-/-</sup> mice.

All authors declare no conflict of interests

Authors contributions:

Park, Shcheynikov, Hong, data acquisition and analysis, Zheng, viral production and delivery, Suh, participated in manuscript drafting, Yule, provided tools, participated in manuscript drafting, Kawai, Ando, Mizutani, Abe, Kiyonari, Seki, Mikoshiba, generated the IRBIT<sup>-/-</sup> mice, participated in manuscript drafting, Shmuel Muallem, directed the study, wrote the manuscript

**Publisher's Disclaimer:** This is a PDF file of an unedited manuscript that has been accepted for publication. As a service to our customers we are providing this early version of the manuscript. The manuscript will undergo copyediting, typesetting, and review of the resulting proof before it is published in its final citable form. Please note that during the production process errors may be discovered which could affect the content, and all legal disclaimers that apply to the journal pertain.

HeLa cells and in ducts isolated from mouse pancreatic and salivary glands. Slc26a6 activity was assayed by measuring intracellular pH, and CFTR activity by measuring  $\text{Cl}^-$  current. Protein interactions were determined by immunoprecipitation analyses.

**Results**—Irbt mediated the synergistic activation of CFTR and Slc26a6 by  $\text{Ca}^{2+}$  and cAMP. In resting cells, Irbt was sequestered by  $\text{InsP}_3$  receptors ( $\text{IP}_3\text{Rs}$ ) in the endoplasmic reticulum. Stimulation of Gs-coupled receptors led to phosphorylation of  $\text{IP}_3\text{Rs}$ , which increased their affinity for  $\text{InsP}_3$  and reduced their affinity for Irbt. Subsequent weak stimulation of Gq-coupled receptors, which led to production of low levels of  $\text{IP}_3$ , caused dissociation of Irbt from  $\text{IP}_3\text{Rs}$  and allowed translocation of Irbt to CFTR and Slc26a6 in the plasma membrane. These processes stimulated epithelial secretion of electrolytes and fluid. These pathways were not observed in pancreatic and salivary glands from Irbt<sup>-/-</sup> or Slc26a6<sup>-/-</sup> mice, or in salivary gland ducts expressing mutant forms of  $\text{IP}_3\text{Rs}$  that could not undergo protein kinase A-mediated phosphorylation.

**Conclusions**—Irbt promotes synergy between the  $\text{Ca}^{2+}$  and cAMP signaling pathways in cultured cells and in pancreatic and salivary ducts from mice. Defects in this pathway could be involved in CF, pancreatitis, or Sjögren's syndrome.

### Keywords

signal transduction; ion and water secretion; fluid; electrolyte

### Background and Aims

Biological systems are regulated by multiple inputs that use several signaling pathways. When operating at full capacity, signaling systems can be highly toxic, as exemplified by  $\text{Ca}^{2+}$ -mediated cellular toxicity<sup>1</sup>. To avoid toxicity, signaling pathways function at 5–10% of maximal capacity, but synergize to generate the maximal response<sup>2</sup>. Hence, synergism is a central concept in biology, yet we do not understand the underlying molecular mechanism. Here, we investigate fluid and  $\text{HCO}_3^-$  secretion by exocrine glands as a model to determine the mechanism of synergism between the ubiquitous  $\text{Ca}^{2+}$  and cAMP signaling pathways.

Epithelial secretion is mediated by basolateral  $\text{HCO}_3^-$  entry mediated by the  $2\text{Na}^+ - 1\text{HCO}_3^-$  cotransporter, NBCe1-B and luminal  $\text{HCO}_3^-$  exit mediated by the concerted activities of the  $1\text{Cl}^-/2\text{HCO}_3^-$  exchanger, slc26a6<sup>3</sup> and the  $\text{Cl}^-$  channel, CFTR<sup>4</sup>. Epithelial secretion is regulated by multiple inputs, most importantly  $\text{Ca}^{2+}$  and cAMP signaling that synergize to generate the full response<sup>2, 5, 6</sup>. Downstream of  $\text{Ca}^{2+}$  and cAMP, ductal fluid and  $\text{HCO}_3^-$  secretion is regulated by two opposing pathways; the WNK/SPAK kinases pathway which inhibits secretion, and the IRBIT/PP1 pathway that stimulates the secretion<sup>7–9</sup>. The WNK kinases are mutated in several forms of hypertension<sup>10</sup>. The SPAK/OSR1 were identified as kinases in the WNKs regulatory pathway<sup>11</sup>. The WNK/SPAK pathway regulates several  $\text{Na}^+$ ,  $\text{K}^+$ ,  $\text{Cl}^-$  and  $\text{HCO}_3^-$  transporters<sup>12</sup>, where the WNKs directly phosphorylate or serve as scaffolds to recruit SPAK that phosphorylate the transporters<sup>9, 13</sup>. Indeed, the WNKs recruit SPAK to NBCe1-B and CFTR, which phosphorylates them to reduce their surface expression thereby inhibiting ductal secretion<sup>7, 8</sup>. IRBIT competes with  $\text{IP}_3$  for binding to the  $\text{IP}_3$  binding pocket in  $\text{IP}_3\text{Rs}$ <sup>14</sup>. NBCe1-B was identified as an IRBIT binding partner that is activated by IRBIT<sup>15</sup>. In ducts, IRBIT recruits PP1 to NBCe1-B and CFTR, reversing phosphorylation by SPAK to increase the transporters surface expression and activate them to set the secretory state<sup>7, 8</sup>.

The intriguing roles of IRBIT in both  $\text{Ca}^{2+}$  signaling through inhibition of the  $\text{IP}_3\text{Rs}$ <sup>14</sup> and in epithelial biology through activation of NBCe1-B and CFTR<sup>7, 8</sup>, prompted us to study a possible role of IRBIT in synergism. We found that IRBIT functions as a third messenger to

mediate synergism between the cAMP and  $\text{Ca}^{2+}$  signaling pathways. Thus, the cAMP and  $\text{Ca}^{2+}$  signaling pathways synergize to fully stimulate CFTR and *slc26a6*. The synergism is mediated by IRBIT and requires PKA-mediated phosphorylation of  $\text{IP}_3\text{Rs}$ . Phosphorylation by PKA increases the interaction of  $\text{IP}_3\text{Rs}$  with  $\text{IP}_3$  and decreases the interaction with IRBIT. Subsequently  $\text{IP}_3$  readily releases IRBIT from  $\text{IP}_3\text{Rs}$  which translocates to CFTR and *slc26a6*, resulting in their activation and epithelial secretion.

## Materials and Methods

### Animals

All animal protocols have been approved by the NIH animal use committee and strictly adhere to all NIH guidelines. Generation of the *slc26a6*<sup>-/-</sup> mice was described before<sup>16</sup>. The details of generating the mice with loxP flanked IRBIT and IRBIT knockout mice are given in supplementary methods and Fig. S1.

### Fluid secretion

Fluid secretion by sealed ducts was measured and analyzed as in<sup>8</sup>. Further details are in supplementary Methods.

### Isolation of parotid cells

Suspension of isolated ducts and acini were prepared by standard procedures<sup>17</sup>, as detailed in the supplement.

### Slc26a6 activity

*slc26a6* activity was analyzed by measuring  $\text{pH}_{in}$  with BCECF as described before<sup>4</sup> and detailed in supplement.

### CFTR current

CFTR  $\text{Cl}^-$  current as detailed before<sup>4</sup>. Solutions and recording conditions are given in supplementary information.

### CFTR activity in duct fragments

Ductal intracellular  $\text{Cl}^-$  was evaluated from MQAE fluorescence. The ducts were loaded with MQAE by 30 min incubation at room temperature in bath solution containing 5 mM MQAE. After mounting the ducts in the perfusion chamber they were washed by perfusion with NaCl-based solution until stabilization of the signal and then the solution was changed to  $\text{NaNO}_3$  based solution. Fluorescence was recorded for at least 3 min to obtain the baseline before stimulation with the indicated concentrations of forskolin and/or carbachol. MQAE fluorescence was recorded at an excitation of 360 nm and light emitted at a wavelength higher than 530 nm was collected. The measured  $\text{Cl}^-/\text{NO}_3^-$  exchange reports CFTR activity.

### Western blot and Co-IP analysis

This was by standard methods as detailed in the supplement.

## Results

### Synergism in ductal fluid secretion

Intralobular pancreatic ducts in primary culture seal within 12–24 hrs and when stimulated with high concentrations of the cAMP generating agonist, Secretin, secrete fluid and electrolytes resulting in expansion of the lumen, yielding a measurement of secretion<sup>8, 18</sup>.

Images of ducts stimulated with 2 and 30nM Secretin or co-stimulation with 2nM Secretin and 1 $\mu$ M carbachol are shown in supplementary movies 1–3. Fig. 1 demonstrates that stimulation of wild-type ducts with 5 $\mu$ M forskolin or 30nM Secretin caused robust fluid secretion. By contrast, stimulation with low concentrations of 0.1 $\mu$ M forskolin, 2nM Secretin or 1 $\mu$ M carbachol resulted in a minimal secretion. Notably, co-stimulation with low concentrations of either secretin or forskolin and carbachol synergize causing robust secretion. Most striking, deletion of IRBIT in mice while partially inhibited the secretion observed with maximal stimulation (about 35%), eliminated the synergistic stimulation, indicating a prominent role of IRBIT in the synergism.

### Generation of IP<sub>3</sub> is required for activation of slc26a6 by IRBIT

To understand the role of IRBIT in mediating the synergism, we first determined that the Cl<sup>-</sup>/2HCO<sub>3</sub><sup>-</sup> exchanger slc26a6 is regulated by the WNK/SPAK and IRBIT/PP1 pathways. Slc26a6-mediated Cl<sup>-</sup>/HCO<sub>3</sub><sup>-</sup> exchange is markedly stimulated by IRBIT (Fig. S2). Slc26a6 is inhibited by an N terminal fragment of WNK1(1–119) and by SPAK (Fig. S3a,b). Further, IRBIT reverses the effects of both WNK1 and SPAK and WNKs and SPAK reduce surface expression of slc26a6 that is reversed by the IRBIT/PP1 pathway (Fig. S3c). This regulation is similar to that occurring with NBCe1-B and CFTR<sup>7, 8</sup> and indicates that the WNKs are scaffolds for SPAK, SPAK acts upstream of WNK and the IRBIT/PP1 pathway stimulates slc26a6 by reversing the effect of SPAK.

To determine how Gq-coupled GPCRs activate slc26a6, HeLa cells expressing slc26a6 were stimulated with 10 $\mu$ M ATP to stimulate native P2Y2 receptors. Fig. 2a and Fig. S4a,b shows that this resulted in marked activation of slc26a6. Importantly, ATP does not stimulate slc26a6 that is fully activated by IRBIT, and the dominant negative IRBIT $\Delta$ PEST and IRBIT $\Delta$ C-C (Fig. S6) prevent activation of slc26a6 by GPCRs. These findings indicate that IRBIT mediates activation of slc26a6 following intense stimulation of Gq-coupled receptors. Gq-coupled receptors generate IP<sub>3</sub> to increase [Ca<sup>2+</sup>]<sub>i</sub>. To determine which of the messengers activate slc26a6, we first increased [Ca<sup>2+</sup>]<sub>i</sub> by inhibition of the SERCA pumps with cyclopiazonic acid (CPA), secondly, treated cells with CPA in 0 Ca<sup>2+</sup> medium to prevent the [Ca<sup>2+</sup>]<sub>i</sub> increase by stimulation with ATP, and thirdly we loaded the cells with the fast Ca<sup>2+</sup> chelator BAPTA. None of these maneuvers prevented activation of slc26a6 following stimulation with ATP (Figs. 2b and S4c,d). By contrast, inhibiting PLC with U73122 prevented activation of slc26a6 by ATP. Importantly, buffering IP<sub>3</sub> with an IP<sub>3</sub> sponge<sup>19</sup> without interfering with cell stimulation completely prevented activation of slc26a6 by ATP. Given that IP<sub>3</sub> dissociates IRBIT from IP<sub>3</sub>Rs<sup>14</sup>, these findings suggest strongly that stimulation by GPCRs involves generation of IP<sub>3</sub> which dissociates IRBIT bound to IP<sub>3</sub>Rs and in turn activates slc26a6. This hypothesis is examined further below.

### Synergism in activation of slc26a6

To further examine activation of slc26a6 by IRBIT and the basis for synergism in epithelial transport, we determined the activation of slc26a6 by cAMP, Gq-coupled receptor and by their combination. Fig. 2c shows that ATP alone maximally activated slc26a6 with EC<sub>50</sub> of about 0.7 $\mu$ M. Forskolin weakly activated slc26a6 even at 10 $\mu$ M. Most notably, Fig. 2c and S5 show that concomitant stimulation with ATP and forskolin markedly synergized to activate slc26a6 with 0.1 $\mu$ M of ATP and forskolin resulting in 50% of maximal activation. Significantly, IRBIT is required for the synergistic activation of slc26a6, as evident by inhibition by dominant negative (Fig. 2c) and knockdown of IRBIT (Fig. S5).

A potential mechanism for the synergism is that cAMP exposure facilitates the interaction of IRBIT with slc26a6, resulting in slc26a6 activation. This was examined directly by determining the effect of the co-stimulation on the Co-IP of IRBIT and slc26a6. Fig. 2d

shows that stimulation with 10 $\mu$ M ATP markedly increased the reciprocal Co-IP of IRBIT and slc26a6, while stimulation with 0.1 $\mu$ M forskolin or 0.3 $\mu$ M ATP had no effect. On the other hand, co-stimulation with 0.1 $\mu$ M forskolin and 0.3 $\mu$ M ATP increased interaction between IRBIT and slc26a6 similar to that observed with maximal stimulation with ATP. Since IRBIT is sequestered by IP<sub>3</sub>Rs, we asked whether the co-stimulation affect the IP<sub>3</sub>Rs-IRBIT interaction. Fig. 2e shows that stimulation with 10 $\mu$ M ATP or with 0.1 $\mu$ M forskolin and 0.3 $\mu$ M ATP nearly completely dissociated the IP<sub>3</sub>Rs-IRBIT complexes.

To extend the finding in Fig. 2 to native tissues, we examined synergism in activation of ductal slc26a6 in wild-type, slc26a6<sup>-/-</sup> and IRBIT<sup>-/-</sup> mice. Most ductal Cl<sup>-</sup>/HCO<sub>3</sub><sup>-</sup> exchange activity is mediated by slc26a6 (<sup>16</sup> and Fig. 3d below). Ducts were stimulated with low carbachol (1 $\mu$ M) to activate the Gq-coupled M3 receptors, and with 0.5 $\mu$ M forskolin to increase cellular cAMP. Figs. 3a,b shows that forskolin and carbachol alone had minimal effect on ductal Cl<sup>-</sup>/HCO<sub>3</sub><sup>-</sup> exchange. However, co-stimulation with carbachol and forskolin synergized to markedly activate ductal Cl<sup>-</sup>/HCO<sub>3</sub><sup>-</sup> exchange. The Co-IP in Fig. 3c revealed increased interaction of *native* slc26a6 and IRBIT in cells stimulated with 100 $\mu$ M carbachol. Importantly, Figs. 3d and 3e show that the synergistic activation of ductal Cl<sup>-</sup>/HCO<sub>3</sub><sup>-</sup> exchange was eliminated in ducts from slc26a6<sup>-/-</sup> and IRBIT<sup>-/-</sup> mice. Moreover, IRBIT is required to maintain basal slc26a6 activity.

### Synergism in activation of CFTR

Epithelial fluid and HCO<sub>3</sub><sup>-</sup> secretion is mediated by the concerted,<sup>4</sup> coupled action of slc26a6 and CFTR<sup>8, 16</sup>. Notably, synergistic fluid secretion by airway epithelia is lost in patients with cystic fibrosis<sup>6</sup>. Yet, surprisingly, neither the synergistic activation of CFTR by Gq- and Gs-coupled receptors, nor the mechanism underlying the synergism has been examined. In Figs. 4 and 5 we investigated the synergistic activation of CFTR in model systems (Fig. 4) and ducts (Fig. 5), and determined the role of IRBIT in the synergism. PKA phosphorylates the CFTR R domain, and maximum PKA-phosphorylation results in full activation. Accordingly, Figs. 4a,b show that CFTR is maximally activated by 5 $\mu$ M forskolin. Stimulation of HeLa cells expressing CFTR with 0.5 $\mu$ M forskolin or with 3 $\mu$ M ATP did not appreciably activate CFTR and stimulation with 10 $\mu$ M ATP only slightly stimulated the channel. By contrast, co-stimulation with 3 $\mu$ M ATP and 0.5 $\mu$ M forskolin synergistically and maximally activated CFTR, whether the cells were stimulated first with ATP or with forskolin. Fig. 4c shows that the dominant negative IRBIT( $\Delta$ C-C) and IRBIT knockdown markedly reduced the synergistic activation of CFTR. Finally, Fig. 4d shows that stimulation with 10 $\mu$ M ATP or co-stimulation with 0.1 $\mu$ M forskolin and 0.3 $\mu$ M ATP increased the interaction between IRBIT and CFTR.

Synergistic activation of CFTR was also observed in salivary gland ducts. CFTR activity in intralobular ducts was measured by the MQAE technique<sup>7, 8</sup>. In Figs. 5a,b the ducts were perfused with HEPES-buffered solution in which Cl<sup>-</sup> was replaced by NO<sub>3</sub><sup>-</sup>, resulting in slow increase in MQAE fluorescence. Stimulation with 2 $\mu$ M forskolin to activate CFTR markedly accelerated the rate of fluorescence increase as a result of CFTR-mediated Cl<sup>-</sup>/NO<sub>3</sub><sup>-</sup> exchange and de-quenching of MQAE fluorescence. As expected, the exchange was inhibited by the CFTR inhibitor CFTR<sub>172</sub><sup>20</sup>. Stimulation with 0.1 $\mu$ M forskolin only slightly increased MQAE fluorescence (Figs. 5a,b). In contrast, the combined stimulation with 0.1 $\mu$ M forskolin and 1 $\mu$ M carbachol activated CFTR almost to the same extent as 2 $\mu$ M forskolin (Figs. 5c,b). The synergistic increase in MQAE fluorescence was inhibited by CFTR<sub>172</sub>. Most significantly, the synergism was eliminated in ducts from IRBIT<sup>-/-</sup> mice (Figs. 5c,b). Finally, Fig. 5d shows that stimulation of the ducts with 100 $\mu$ M carbachol increased the interaction between CFTR and IRBIT. Hence, it is clear that IRBIT mediates the synergistic activation of expressed and native CFTR by the cAMP and Ca<sup>2+</sup> signaling pathways.

## The synergism is mediated by PKA phosphorylation of the IP<sub>3</sub>Rs

To explore the molecular mechanism of the synergism we reasoned that given that IRBIT and IP<sub>3</sub> act on the same site<sup>14</sup>, the increased affinity of the PKA-phosphorylated IP<sub>3</sub>Rs to IP<sub>3</sub><sup>21-23</sup> may facilitate the release of IRBIT from the IP<sub>3</sub>Rs and subsequent binding to CFTR and slc26a6<sup>14</sup>. To test this hypothesis, we used IP<sub>3</sub>R1 in which the PKA-phosphorylated sites S1589/S1755 were mutated to either Ala (AA) or to the phosphomimetic Glu (EE)<sup>22</sup> and tested how the mutations affected binding and release of IRBIT to IP<sub>3</sub>Rs. The reciprocal Co-IP in Fig. 6a shows that the AA mutant increases and the EE mutant decreases interaction of IRBIT with IP<sub>3</sub>R1. Moreover, 0.3μM IP<sub>3</sub> dissociated minimal amount of IRBIT from the AA mutant, whereas the same concentration of IP<sub>3</sub> nearly completely dissociated IRBIT from IP<sub>3</sub>R1.

Next, we used these IP<sub>3</sub>R1 mutants to test the role of PKA-mediated phosphorylation in the synergistic activation of CFTR and slc26a6 in model system and *in vivo*. The traces and summary in Fig. 6b show that expression of IP<sub>3</sub>R1(AA) eliminated the synergistic activation of slc26a6. Fig. 6b and Fig. S7a,b show that expression of IP<sub>3</sub>R1(EE), while not further affecting the synergism (Fig. 6b), facilitated activation of slc26a6 by low concentrations of forskolin (Fig. S7a,b). Similar results were obtained with CFTR. Figs. 6d, 6f and S7c,d show that expression of IP<sub>3</sub>R1(AA) markedly reduced the rate and extent of synergistic activation of CFTR, while the IP<sub>3</sub>R1(EE) mutant increased synergistic activation of CFTR and facilitated activation of CFTR by forskolin alone.

To determine the role of IP<sub>3</sub>Rs phosphorylation *in vivo*, IP<sub>3</sub>R1 and IP<sub>3</sub>R1(AA) packaged in adenoviruses that co-expressed GFP were delivered to mouse submandibular salivary gland ducts by retrograde infusion through the opening of the main duct to the oral cavity, (image in Fig. 6). Seven days was allowed after infection for recovery of the gland from any potential inflammation<sup>24</sup>, the ducts were isolated and used to assay synergistic activation of slc26a6 and CFTR. Fig. 6c (slc26a6) and 6e (CFTR) and the corresponding summaries show that IP<sub>3</sub>R1(AA) nearly eliminated the synergistic activation of the two ductal transporters.

## Discussion

Physiological responses are controlled by multiple inputs that activate several signaling pathways. The signaling outputs are integrated by crosstalk and synergism among the pathways. Prime examples are the crosstalk and synergism between Ca<sup>2+</sup> and cAMP signaling. For example, the cAMP pathway augments Ca<sup>2+</sup> signals by phosphorylation of IP<sub>3</sub>Rs<sup>25</sup> and the Ca<sup>2+</sup> signal itself activates Ca<sup>2+</sup>-dependent adenylyl cyclases<sup>26</sup>. Ca<sup>2+</sup> and cAMP signaling synergize in many biological processes, including epithelial secretion<sup>2, 5, 6</sup>. Crosstalk coordinates and integrates the inputs of signaling pathways. Synergism confers tighter control and buffering of the physiological response and avoidance of toxicity as a result of intense activation of the pathways.

Signaling crosstalk has been extensively studied, but we know very little about the molecular mechanism responsible for synergism. The aim of the present work is to provide a framework to understand the molecular mechanism of synergism by studying exocrine gland fluid and HCO<sub>3</sub><sup>-</sup> secretion. We found synergistic activation of CFTR (Figs. 4, 5) and slc26a6 (Figs. 2, 3) and consequently of epithelial fluid secretion (Fig. 1). We further showed that IRBIT functions as a third messenger to mediate the synergism. The model in Fig. 7 illustrates the role of IRBIT in synergism and activation of epithelial fluid and HCO<sub>3</sub><sup>-</sup> secretion. In the resting state the WNK and SPAK kinases phosphorylate NBCe1-B, slc26a6 and CFTR to promote their endocytosis<sup>13</sup> or inhibit their exocytosis<sup>12</sup> and thus reduce their surface expression to establish the basal secretory state. In the basal state, IRBIT is sequestered by binding to IP<sub>3</sub>Rs (Fig. 2e) that are expressed at high level at the apical pole

in both duct (left image) and acinar (right image) cells. The apical pole is also the major localization of all  $\text{Ca}^{2+}$  and cAMP signaling complexes.<sup>27</sup> For example, CCK and muscarinic receptors which generate  $\text{IP}_3$ , together with VIP receptors complexes which generate cAMP are concentrated in the apical pole, thus ensuring production of cAMP and  $\text{IP}_3$  at the site where the  $\text{IP}_3$ Rs are concentrated.

Cell stimulation with physiologically relevant concentrations of cAMP (Gs-coupled) and  $\text{IP}_3$  (Gq-coupled) generating agonists lead to phosphorylation of  $\text{IP}_3$ Rs by PKA. This event increases the functional affinity of  $\text{IP}_3$ R for  $\text{IP}_3$ , while reducing their apparent affinity for IRBIT. The low concentration of  $\text{IP}_3$  is now rendered sufficient to dissociate IRBIT from  $\text{IP}_3$ Rs at the ER and allow its transfer to slc26a6 and CFTR at the plasma membrane (Figs. 2–6) Hence, IRBIT functions as a messenger to transfer the stimulus from the ER to the plasma membrane. IRBIT has two effects on the transporters. First, IRBIT recruits PP1 to the transporters to dephosphorylate them at the SPAK site and thus restore their surface expression. Second, IRBIT activates the transporters by increasing  $\text{Cl}^-/\text{HCO}_3^-$  exchange by slc26a6 (Fig. 2) and the open probability of CFTR<sup>8</sup>. Activation of the transporters can occur by removal of an inhibitory domain or by facilitating the interaction between the CFTR R domain and the slc26a6 STAS domain that we<sup>4</sup> and others<sup>28</sup> showed to mutually activate the transporters. IRBIT activates NBCe1-B by preventing autoinhibition by the NBCe1-B N terminus<sup>8, 15</sup> that also complements stimulation by  $\text{PIP}_2$  and prevents inhibition by SPAK<sup>29</sup> and cytoplasmic  $\text{Mg}^{2+30}$ . The synergistic activation of the key luminal  $\text{Cl}^-$  and  $\text{HCO}_3^-$  transporters and of the basolateral  $\text{HCO}_3^-$  transporter by IRBIT result in stimulated epithelial fluid and  $\text{HCO}_3^-$  secretion.

Notably, the synergistic mechanism described here likely functions in other physiological situations. Recently, it was reported that the glucagon-mediated gluconeogenic program involves interactions between cAMP and  $\text{Ca}^{2+}$  signaling at the level of  $\text{IP}_3$ Rs to modulate hepatic glucose production under both fasting conditions and in diabetes<sup>31</sup>. Specifically, glucagon-triggered PKA-mediated phosphorylation of  $\text{IP}_3$ Rs facilitates  $\text{Ca}^{2+}$  mobilization and activation of calcineurin that dephosphorylates the CREB co-activator CRTC<sup>31</sup>. It will be of interest to determine if IRBIT is involved in this system as an activator of calcineurin or in mediating the interaction of calcineurin with CRTC2.

## Supplementary Material

Refer to Web version on PubMed Central for supplementary material.

## Acknowledgments

This work was funded by Intramural Research grant ZIA-DE000735.

## Abbreviations

<b>IRBIT</b>	$\text{IP}_3$ receptor-binding protein released with $\text{IP}_3$
<b>WNK</b>	With No Lysine
<b>SPAK</b>	Ste20-related proline alanine rich kinase
<b>PP1</b>	Protein phosphatase 1
<b><math>\text{IP}_3</math>Rs</b>	$\text{IP}_3$ receptors
<b>slc26a6</b>	Solute carrier family 26, member 6

## References

1. Berridge MJ. Calcium signalling remodelling and disease. *Biochemical Society transactions*. 2012; 40:297–309. [PubMed: 22435804]
2. Lee MG, Ohana E, Park HW, et al. Molecular mechanism of pancreatic and salivary gland fluid and HCO<sub>3</sub> secretion. *Physiological reviews*. 2012; 92:39–74. [PubMed: 22298651]
3. Shcheynikov N, Wang Y, Park M, et al. Coupling modes and stoichiometry of Cl<sup>-</sup>/HCO<sub>3</sub><sup>-</sup> exchange by slc26a3 and slc26a6. *The Journal of general physiology*. 2006; 127:511–24. [PubMed: 16606687]
4. Ko SB, Zeng W, Dorwart MR, et al. Gating of CFTR by the STAS domain of SLC26 transporters. *Nat Cell Biol*. 2004; 6:343–50. [PubMed: 15048129]
5. Burnham DB, Williams JA. Stimulus-secretion coupling in pancreatic acinar cells. *Journal of pediatric gastroenterology and nutrition*. 1984; 3 (Suppl 1):S1–10. [PubMed: 6094780]
6. Choi JY, Joo NS, Krouse ME, et al. Synergistic airway gland mucus secretion in response to vasoactive intestinal peptide and carbachol is lost in cystic fibrosis. *The Journal of clinical investigation*. 2007; 117:3118–27. [PubMed: 17853942]
7. Yang D, Li Q, So I, Huang CL, et al. IRBIT governs epithelial secretion in mice by antagonizing the WNK/SPAK kinase pathway. *The Journal of clinical investigation*. 2011; 121:956–65. [PubMed: 21317537]
8. Yang D, Shcheynikov N, Zeng W, et al. IRBIT coordinates epithelial fluid and HCO<sub>3</sub><sup>-</sup> secretion by stimulating the transporters pNBC1 and CFTR in the murine pancreatic duct. *J Clin Invest*. 2009; 119:193–202. [PubMed: 19033647]
9. Park S, Hong JH, Ohana E, et al. The WNK/SPAK and IRBIT/PP1 Pathways in Epithelial Fluid and Electrolyte Transport. *Physiology*. 2012; 27:291–9. [PubMed: 23026752]
10. Wilson FH, Disse-Nicodeme S, Choate KA, et al. Human hypertension caused by mutations in WNK kinases. *Science*. 2001; 293:1107–12. [PubMed: 11498583]
11. Gagnon KB, Delpire E. Molecular physiology of SPAK and OSR1: two Ste20-related protein kinases regulating ion transport. *Physiological reviews*. 2012; 92:1577–617. [PubMed: 23073627]
12. McCormick JA, Ellison DH. The WNKs: atypical protein kinases with pleiotropic actions. *Physiological reviews*. 2011; 91:177–219. [PubMed: 21248166]
13. He G, Wang HR, Huang SK, et al. Intersectin links WNK kinases to endocytosis of ROMK1. *The Journal of clinical investigation*. 2007; 117:1078–87. [PubMed: 17380208]
14. Ando H, Mizutani A, Kiefer H, et al. IRBIT suppresses IP<sub>3</sub> receptor activity by competing with IP<sub>3</sub> for the common binding site on the IP<sub>3</sub> receptor. *Mol Cell*. 2006; 22:795–806. [PubMed: 16793548]
15. Shirakabe K, Priori G, Yamada H, et al. IRBIT, an inositol 1,4,5-trisphosphate receptor-binding protein, specifically binds to and activates pancreas-type Na<sup>+</sup>/HCO<sub>3</sub><sup>-</sup> cotransporter 1 (pNBC1). *Proc Natl Acad Sci U S A*. 2006; 103:9542–7. [PubMed: 16769890]
16. Wang Y, Soyombo AA, Shcheynikov N, et al. Slc26a6 regulates CFTR activity in vivo to determine pancreatic duct HCO<sub>3</sub><sup>-</sup> secretion: relevance to cystic fibrosis. *The EMBO journal*. 2006; 25:5049–57. [PubMed: 17053783]
17. Lee MG, Schultheis PJ, Yan M, et al. Membrane-limited expression and regulation of Na<sup>+</sup>-H<sup>+</sup> exchanger isoforms by P<sub>2</sub> receptors in the rat submandibular gland duct. *The Journal of physiology*. 1998; 513 ( Pt 2):341–57. [PubMed: 9806987]
18. Ishiguro H, Steward MC, Wilson RW, et al. Bicarbonate secretion in interlobular ducts from guinea-pig pancreas. *The Journal of physiology*. 1996; 495 ( Pt 1):179–91. [PubMed: 8866361]
19. Uchiyama T, Yoshikawa F, Hishida A, et al. A novel recombinant hyperaffinity inositol 1,4,5-trisphosphate (IP<sub>3</sub>) absorbent traps IP<sub>3</sub>, resulting in specific inhibition of IP<sub>3</sub>-mediated calcium signaling. *The Journal of biological chemistry*. 2002; 277:8106–13. [PubMed: 11741904]
20. Ma T, Thiagarajah JR, Yang H, et al. Thiazolidinone CFTR inhibitor identified by high-throughput screening blocks cholera toxin-induced intestinal fluid secretion. *The Journal of clinical investigation*. 2002; 110:1651–8. [PubMed: 12464670]
21. Wagner LE, Li WH, Yule DI. Phosphorylation of type-1 inositol 1,4,5-trisphosphate receptors by cyclic nucleotide-dependent protein kinases: a mutational analysis of the functionally important



- sites in the S2+ and S2- splice variants. *The Journal of biological chemistry*. 2003; 278:45811-7. [PubMed: 12939273]
22. Wagner LE, Li WH, Joseph SK, et al. Functional consequences of phosphomimetic mutations at key cAMP-dependent protein kinase phosphorylation sites in the type 1 inositol 1,4,5-trisphosphate receptor. *The Journal of biological chemistry*. 2004; 279:46242-52. [PubMed: 15308649]
  23. Wagner LE, Joseph SK, Yule DI. Regulation of single inositol 1,4,5-trisphosphate receptor channel activity by protein kinase A phosphorylation. *The Journal of physiology*. 2008; 586:3577-96. [PubMed: 18535093]
  24. Zheng C, Goldsmith CM, Mineshiba F, et al. Toxicity and biodistribution of a first-generation recombinant adenoviral vector, encoding aquaporin-1, after retroductal delivery to a single rat submandibular gland. *Human gene therapy*. 2006; 17:1122-33. [PubMed: 17069536]
  25. Yule DI, Betzenhauser MJ, Joseph SK. Linking structure to function: Recent lessons from inositol 1,4,5-trisphosphate receptor mutagenesis. *Cell calcium*. 2010; 47:469-79. [PubMed: 20510450]
  26. Halls ML, Cooper DM. Regulation by Ca<sup>2+</sup>-signaling pathways of adenylyl cyclases. *Cold Spring Harbor perspectives in biology*. 2011; 3:a004143. [PubMed: 21123395]
  27. Kiselyov K, Wang X, Shin DM, et al. Calcium signaling complexes in microdomains of polarized secretory cells. *Cell calcium*. 2006; 40:451-9. [PubMed: 17034849]
  28. Bertrand CA, Zhang R, Pilewski JM, et al. SLC26A9 is a constitutively active, CFTR-regulated anion conductance in human bronchial epithelia. *The Journal of general physiology*. 2009; 133:421-38. [PubMed: 19289574]
  29. Hong JH, Yang D, Shcheynikov N, et al. Convergence of IRBIT, PIP<sub>2</sub> and the WNK/SPAK kinases in regulation of the Na<sup>+</sup>-HCO<sub>3</sub><sup>-</sup> co-transporters family. *Proc Natl Acad Sci U S A*. 2013 In Press.
  30. Yamaguchi S, Ishikawa T. IRBIT reduces the apparent affinity for intracellular Mg(2)(+) in inhibition of the electrogenic Na(+)-HCO(3)(-) cotransporter NBCe1-B. *Biochemical and biophysical research communications*. 2012; 424:433-8. [PubMed: 22771795]
  31. Wang Y, Li G, Goode J, et al. Inositol-1,4,5-trisphosphate receptor regulates hepatic gluconeogenesis in fasting and diabetes. *Nature*. 2012; 485:128-32. [PubMed: 22495310]

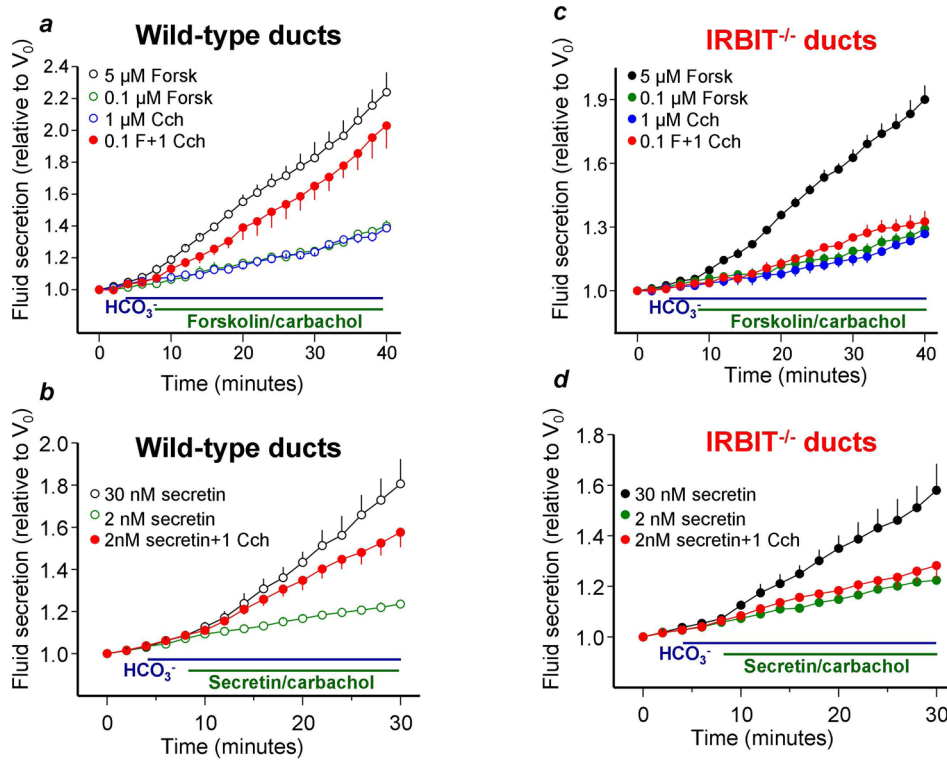


**Fig. 1. IRBIT is required for synergistic activation of ductal fluid secretion**

(a, b): Fluid secretion in pancreatic ducts from wild-type mice was measured in sealed ducts in  $\text{HCO}_3^-$ -buffered media and stimulated with  $5\mu\text{M}$  forskolin or  $30\text{nM}$  secretin (open black circles), low concentration of  $0.1\mu\text{M}$  forskolin or  $2\text{nM}$  secretin (open green circles),  $1\mu\text{M}$  carbachol (open blue circles) and the combination of  $0.1\mu\text{M}$  forskolin or  $2\text{nM}$  secretin and  $1\mu\text{M}$  carbachol (red close circles). (c, d): Same as (a, b), except that ducts are from  $\text{IRBIT}^{-/-}$  mice that were stimulated with  $5\mu\text{M}$  forskolin or  $30\text{nM}$  secretin (close black circles),  $0.1\mu\text{M}$  forskolin or  $2\text{nM}$  secretin (close green circles),  $1\mu\text{M}$  carbachol (close blue circles) and the combination of  $0.1\mu\text{M}$  forskolin or  $2\text{nM}$  secretin and  $1\mu\text{M}$  carbachol (close red circles). The results are mean  $\pm$  S.E.M of 4–6 experiments. The secretory rates with  $5\mu\text{M}$  forskolin and  $30\text{nM}$  secretin between 12–40/30 min for wild-type and  $\text{IRBIT}^{-/-}$  ducts and with low forskolin or secretin +  $1\mu\text{M}$  carbachol between 14–40/30 min for wild-type ducts are different from the rates at the low agonist concentrations at  $P < 0.05$  or better. Stimulation with  $0.1\mu\text{M}$  forskolin or  $2\text{nM}$  secretin +  $1\mu\text{M}$  carbachol are not different from the additive response in  $\text{IRBIT}^{-/-}$  ducts.

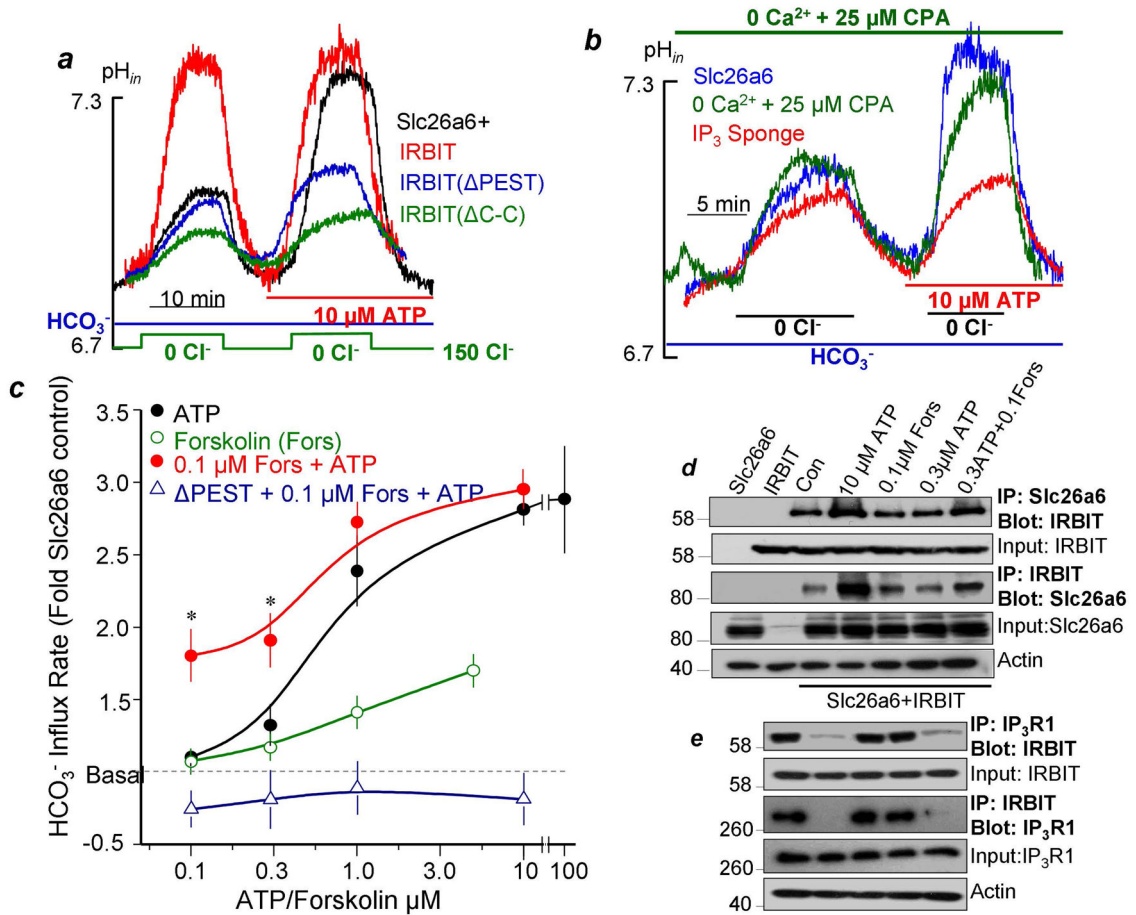


**Fig. 2. IRBIT mediates synergistic activation of slc26a6 by GPCRs which depends on generation of IP<sub>3</sub>**

All experiments with transfected slc26a6 and the indicated constructs were performed in HeLa cells.  $\text{Cl}^-/\text{HCO}_3^-$  exchange was measured in cells bathed in  $\text{HCO}_3^-$ -buffered media that was alternated by perfusion between 150 and 0mM  $\text{Cl}^-$ . **(a)**: Cells were transfected with slc26a6 alone, with IRBIT or with the dominant negatives IRBIT( $\Delta$ PEST) or IRBIT( $\Delta$ C-C) and  $\text{Cl}^-/\text{HCO}_3^-$  exchange activity was measured before and after stimulation of the P2Y2 receptors with 10 $\mu\text{M}$  ATP. **(b)**: For details of each condition see legend of Fig. S4. A sustained increase in  $\text{Ca}^{2+}$ , elimination of the  $\text{Ca}^{2+}$  increase and loading with BAPTA has no effect of activation of slc26a6 by ATP. Attenuation of IP<sub>3</sub> production by inhibiting PLC with U73211 and scavenging IP<sub>3</sub> with IP<sub>3</sub> sponge inhibited activation of slc26a6 by ATP. **(c)**: Synergistic activation of slc26a6 by 0.1 $\mu\text{M}$  forskolin and 0.1 and 0.3 $\mu\text{M}$  ATP. HeLa cells transfected with slc26a6 or slc26a6 and IRBIT( $\Delta$ PEST) were stimulated with ATP alone (close black circles), forskolin alone (open green circles) or with 0.1 $\mu\text{M}$  forskolin and the various concentrations of ATP (close red circles and open purple triangles). The results are the mean $\pm$ S.E.M of 4–6 experiments. **(d, e)**: Synergistic translocation of IRBIT to slc26a6 and dissociation of IRBIT-IP<sub>3</sub>R1 complexes. HeLa cells transfected with slc26a6 and IRBIT **(d)** or IRBIT and IP<sub>3</sub>R1 **(e)** were treated with vehicle (control) or stimulated for 5 min at 37 °C with 10 or 0.3 $\mu\text{M}$  ATP, 0.1 $\mu\text{M}$  forskolin or 0.1 $\mu\text{M}$  forskolin and 0.3 $\mu\text{M}$  ATP. The controls are cells transfected with slc26a6 or IRBIT alone. The level of actin was used to adjust input and as loading control.

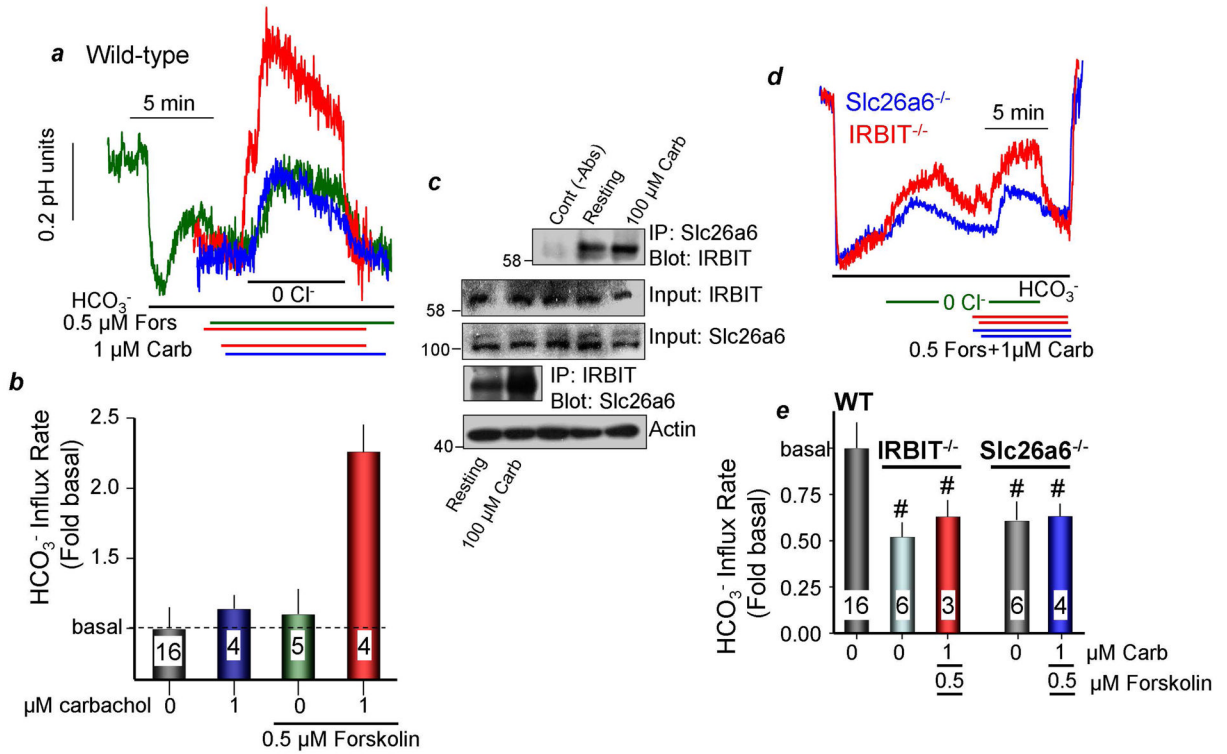


**Fig. 3. IRBIT mediates synergistic activation of Cl<sup>-</sup>/HCO<sub>3</sub><sup>-</sup> exchange by GPCRs in isolated ducts**

**(a, b):** Synergistic activation of Cl<sup>-</sup>/HCO<sub>3</sub><sup>-</sup> exchange activity in isolated parotid ducts. Acutely isolated parotid gland ducts from wild-type mice were used to measure Cl<sup>-</sup>/HCO<sub>3</sub><sup>-</sup> exchange in response to 1 μM carbachol, 0.5 μM forskolin or forskolin and carbachol, as indicated. **(b)** is the mean ± S.E.M. **(c):** Synergistic translocation of IRBIT to slc26a6 *in vivo*. Cells isolated from the parotid glands were treated with vehicle (resting) or 100 μM carbachol for 5 min to maximize generation of IP<sub>3</sub>. The lysates were used to assay for the reciprocal Co-IP of slc26a6 and IRBIT. The controls are lysate without the primary antibodies. Actin was used to adjust initial input. **(d, e):** The synergistic activation of slc26a6 is absent in ducts from IRBIT<sup>-/-</sup> mice. Ducts isolated from slc26a6<sup>-/-</sup> mice show no synergism in activation of Cl<sup>-</sup>/HCO<sub>3</sub><sup>-</sup> exchange, indicating that the synergistic activity in **(a, b)** is of slc26a6. Deletion of IRBIT reduced the basal and eliminated the synergistic activation of Cl<sup>-</sup>/HCO<sub>3</sub><sup>-</sup> exchange by carbachol and forskolin. **(e)** is the mean ± S.E.M. Basal HCO<sub>3</sub><sup>-</sup> transport rate was 0.082 ± 0.004 pH units/min. # denotes P < 0.05 or better.

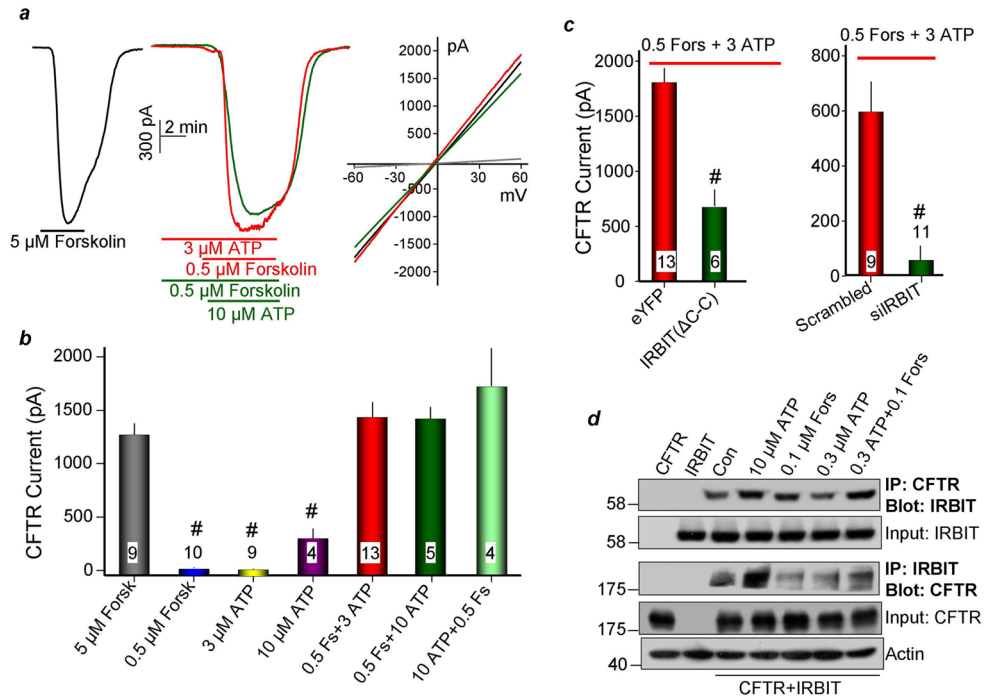


**Fig. 4. IRBIT mediates synergistic activation of CFTR by GPCRs in model system**  
**(a, b):** Synergistic activation of CFTR by 0.5μM forskolin and 3μM ATP. **(a)** shows sample traces and **(b)** is the mean±S.E.M. The cAMP-activated CFTR was transfected in HeLa cells and the current was measured in cells stimulated with 5μM forskolin, 3μM ATP and then 0.5μM forskolin or 0.5μM forskolin and then 10μM ATP. The I/V curves show typical CFTR I/V and the current was blocked by the CFTR inhibitor CFTR<sub>172</sub>. **(c):** the dominant negative IRBIT(ΔC-C) and siIRBIT eliminate the synergism. **(d):** Synergistic translocation of IRBIT to CFTR. HeLa cells transfected with CFTR and IRBIT were treated with vehicle (control) or stimulated for 5 min at 37 °C with 10 or 0.3μM ATP, 0.1μM forskolin or 0.1μM forskolin and 0.3mM ATP. The controls are cells transfected with CFTR or IRBIT alone. Actin was used to adjust for initial input.

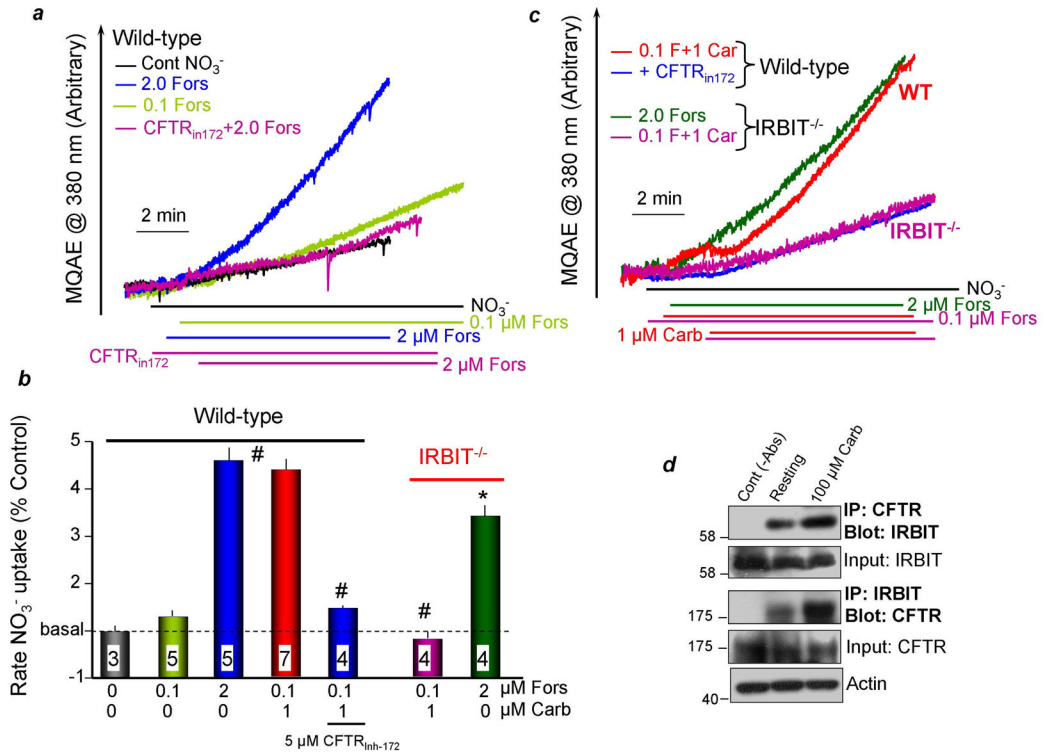


**Fig. 5. IRBIT mediates synergistic activation of ductal CFTR by GPCRs**  
 (a–c): Synergistic activation of CFTR-mediated  $\text{Cl}^-/\text{NO}_3^-$  exchange in isolated ducts is absent in IRBIT $^{-/-}$  ducts. In (a), isolated parotid ducts from wild-type mice were loaded with MQAE. The ducts were perfused with HEPES-buffered media containing 150mM  $\text{Cl}^-$  or  $\text{NO}_3^-$ , as indicated. The cells were stimulated with 2 $\mu\text{M}$  forskolin (blue and magenta) or 0.1 $\mu\text{M}$  forskolin (light green) and treated with 5 $\mu\text{M}$   $\text{CFTR}_{172}$  (magenta). In (c) ducts from wild-type ducts were stimulated with 0.1 $\mu\text{M}$  forskolin and 1 $\mu\text{M}$  carbachol (red, blue) and treated with 5 $\mu\text{M}$   $\text{CFTR}_{172}$  (blue). Parotid ducts from IRBIT $^{-/-}$  mice were stimulated with 2 $\mu\text{M}$  forskolin (green) or 0.1 $\mu\text{M}$  forskolin and 1 $\mu\text{M}$  carbachol (magenta). (b) is the mean  $\pm$ S.E.M. (d), Synergistic translocation of IRBIT to CFTR *in vivo*. Cells isolated from the parotid glands were treated with vehicle (resting) or stimulated with 100 $\mu\text{M}$  carbachol for 5 min. The lysates were used to assay for the reciprocal Co-IP of slc26a6 and IRBIT. The controls are lysate without the primary antibodies. Actin was used to adjust for initial input.

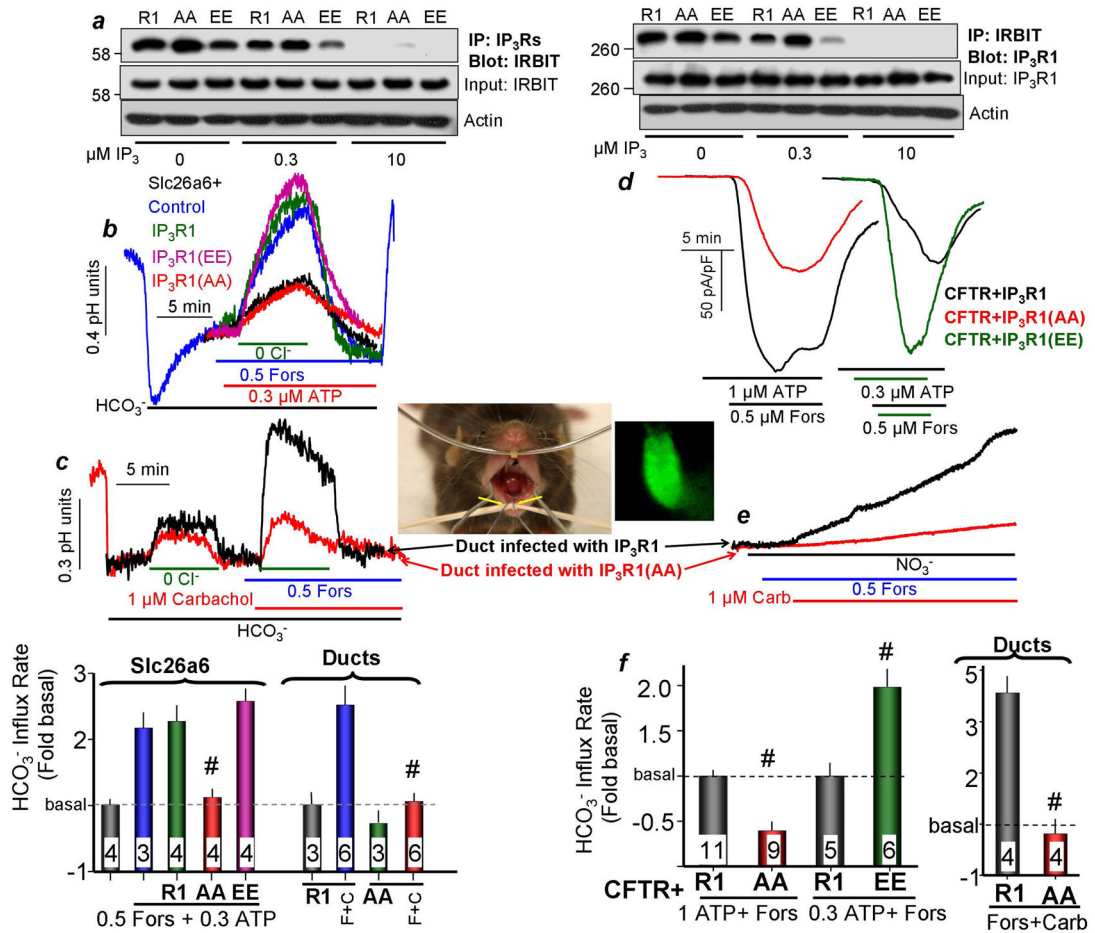


**Fig. 6. PKA-mediated phosphorylation of IP<sub>3</sub>Rs facilitates IRBIT release and translocation to slc26a6 and CFTR**

(a): IP<sub>3</sub>R PKA phosphorylation mutants affect IRBIT interaction with IP<sub>3</sub>Rs. The PKA phosphorylated IP<sub>3</sub>R1 S1589/S1755 sites were mutated to Ala (AA) or Glu (EE) to mimic the unphosphorylated and the phosphorylated forms, respectively. The wild-type and mutant IP<sub>3</sub>R1 were co-transfected with IRBIT and the lysates were incubated on ice for 10 min with 0, 0.3 or 10 μM IP<sub>3</sub> before addition of the antibodies to start the Co-IP. Note that the AA mutant weakens while the EE mutant facilitates IRBIT release from IP<sub>3</sub>Rs. (b): Example traces showing that IP<sub>3</sub>R1 AA mutant inhibits while the EE mutant facilitates the synergistic activation of slc26a6 by GPCRs. The cells were stimulation with 0.5 μM forskolin and 0.3 μM ATP. The columns bracketed by slc26a6 show the mean ± S.E.M. All cells are transfected with slc26a6 and the empty vector or the indicated IP<sub>3</sub>R1 mutant. Basal slc26a6-mediated HCO<sub>3</sub><sup>-</sup> transport rate was measured in unstimulated cells and was 0.061 ± 0.003 pH units/min. (d, f): The IP<sub>3</sub>R1 AA mutant inhibits while the EE mutant facilitates the synergistic activation of CFTR by GPCRs. CFTR current was measured in response to stimulation with 0.5 μM forskolin and 1 μM ATP or 0.3 μM ATP, as indicated. The left columns in (f) are the mean ± S.E.M. of cells expressing CFTR and the indicated IP<sub>3</sub>R1 mutants. (c, e, f): The IP<sub>3</sub>R1 AA mutant eliminates synergistic activation of slc26a6 and CFTR *in vivo*. Adenoviruses carrying GFP and wild-type or AA mutant IP<sub>3</sub>R1 were infused retrogradely through the duct into the submandibular glands (yellow arrows). After 7 days, ducts were isolated and infected ducts were identified by GFP fluorescence (see an example image of GFP-expressing duct). The ducts were loaded with BCECF (c) or with MQAE (e)

to assay synergistic activation of slc26a6 (**c**) or CFTR (**e, f**) in response to stimulation with  $1\mu\text{M}$  carbachol and  $0.5\mu\text{M}$  forskolin. The columns in (**c** and **f**) bracketed by “ducts” are the  $\text{mean}\pm\text{S.E.M}$  with isolated ducts. # denotes  $P<0.001$  relative to the respective R1.



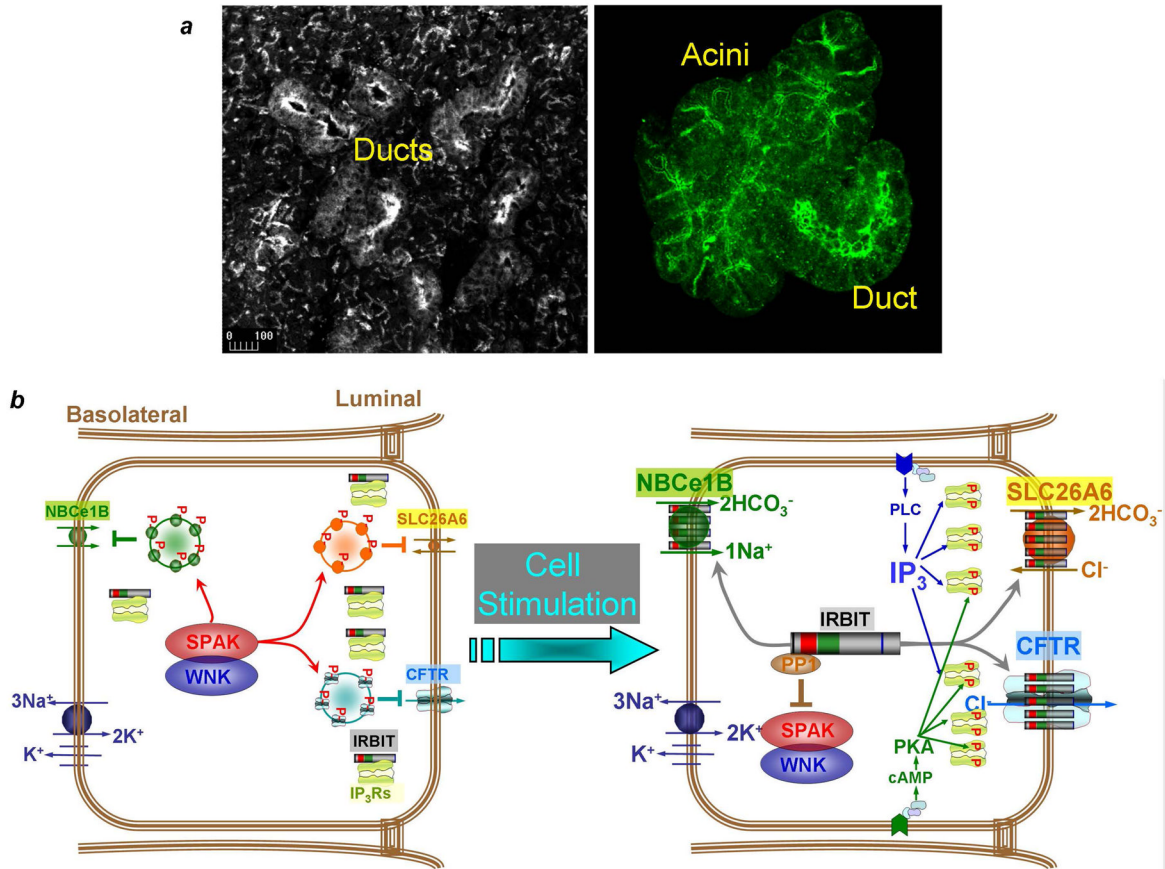


**Fig. 7. A model depicting the molecular mechanism of synergism in epithelial fluid and electrolyte secretion, related to discussion**

(a): The images show high level of IP<sub>3</sub>Rs in the apical pole of the submandibular ducts and acini in tissue sections (left image) and isolated cells (right image). Cell isolation does not disrupt clustering of IP<sub>3</sub>Rs at the apical pole.

(b): In the resting state the WNK kinases function as scaffolds to recruit SPAK to the transporters. SPAK phosphorylates CFTR and slc26a6 (marked by red p) to reduce their surface expression by promoting their endocytosis or reducing their exocytosis<sup>7</sup>. In the absence of IP<sub>3</sub> and when the IP<sub>3</sub>Rs are not phosphorylated by PKA, most IRBIT is sequestered by IP<sub>3</sub>Rs at the apical pole (panel a). Physiological stimulation with both Gq- and Gs-coupled receptors generates cAMP and IP<sub>3</sub>. cAMP activates PKA that phosphorylates the IP<sub>3</sub>Rs at specific sites<sup>22</sup>. This increases the affinity of the IP<sub>3</sub>Rs to IP<sub>3</sub> to facilitate dissociation of IRBIT from IP<sub>3</sub>Rs and its translocation to slc26a6 and CFTR. Hence, IRBIT functions as a third messenger to transmit the stimulated state to CFTR and slc26a6 that are minimally stimulated by the low physiological cAMP concentration. IRBIT does so by recruiting PPI to the transporters to dephosphorylate them and increase their surface expression and then activates them.